J Appl Physiol 92: 2521–2528, 2002.
First published January 4, 2002; 10.1152/japplphysiol.01163.2001.

Comparison of transient otoacoustic emission responses from neonatal and adult ears

GIOVANNA ZIMATORE,[1] STAVROS HATZOPOULOS,[2] ALESSANDRO GIULIANI,[3] ALESSANDRO MARTINI,[2] AND ALFREDO COLOSIMO[1]
[1]*Department of Human Physiology and Pharmacology, University of Rome La Sapienza, 00185 Rome;* [2]*Center of Bioacoustics, University of Ferrara, 44100 Ferrara; and* [3]*Istituto Superiore di Sanità, TCE Laboratory, 00161 Rome, Italy*

Received 26 November 2001; accepted in final form 31 December 2001

Zimatore, Giovanna, Stavros Hatzopoulos, Alessandro Giuliani, Alessandro Martini, and Alfredo Colosimo. Comparison of transient otoacoustic emission responses from neonatal and adult ears. *J Appl Physiol* 92: 2521–2528, 2002. First published January 4, 2002; 10.1152/japplphysiol.01163.2001.—Transient otoacoustic emission (TEOAE) responses from neonatal (age: 48 h) and adult subjects (age: 26.6 ± 10.0 yr) were analyzed by the combined use of recurrence quantification analysis and singular value decomposition. The data from the two age groups showed significant differences and similarities. The neonatal responses presented less deterministic structures than those of the adults in terms of recurrent dynamic features. In both data sets, the same high level of individual specific dynamic features was observed. The results from the singular value decomposition analysis suggest that a large percentage of variability in all of the analyzed responses can be explained by four to five essential modes. This number is lower than that observed in simulated TEOAE responses generated by a five-component gammatone model. A possible explanation is presented, based on simple instrumental and morphoanatomic considerations.

hearing physiology; otoacoustic emissions; nonlinear methods; principal component analysis; singular value decomposition; gammatones

THE TRANSIENTLY OTOACOUSTIC emission (TEOAE) responses are generated by the movement of outer hair cells (OHCs) on the organ of Corti, when the auditory periphery is stimulated by an acoustic click. In mammals, the OHCs, together with the inner hair cells, the pillar cells, and the tectorial membrane represent a sophisticated apparatus that allows recognition and analysis of the incoming acoustical vibration in the range from 20 Hz to 20 kHz. The TEOAEs are present in 100% of normal hearing subjects and constitute an expression of a normal cochlear functionality (28).

The information contained in the structure of the TEOAE responses could reveal the details of many auditory processes concerning not only the auditory periphery but the central nervous system as well. In fact, the central nervous system modulates the function of OHCs and inner hair cells through medial and lateral afferent fibers (22). These facts have led to new procedures, based on the acquisition of TEOAE responses, which aim to establish the relationship between cochlear mechanics and the effects of the olivocochlear system (17, 23, 24).

The data in the literature indicate that the neonatal TEOAE responses, with respect to the adult ones, are characterized by *1*) a large signal amplitude (26, 28); *2*) a wider and more uniform spectrum, shifted occasionally toward higher frequencies (25); and *3*) a large intrasubject variability (for newborn subjects and children up to ~6 yr of age) (11, 19, 23).

In a previous study (38), our laboratory provided a detailed description of the dynamic properties of TEOAEs from adult subjects by using two techniques: the recurrence quantification analysis (RQA) and the principal component analysis (PCA). In the present study, we extend those results by applying the same analytic strategy to newborn subjects as a means of acquiring an additional insight into the dynamic characteristics of the TEOAEs through a systematic comparison of two different age classes: newborns and adults.

From a practical viewpoint, our aim was to *1*) investigate the age-related features of TEOAEs from a dynamic perspective; *2*) define some general criteria to compare TEOAE responses recorded under quite different conditions; and *3*) provide the basis for a future investigation of preterm and full-term newborns, as well as for a comparison between human and other mammalian signals.

It is worth stressing that the analytic methods we used include a standardization procedure that eliminates any effect of the signal amplitude on the dynamics. This allowed us to focus only on the order (time)-dependent features of the TEOAE responses and to classify them from an essentially statistical viewpoint. In the common practice of the study of complex signals, this is considered a basic step toward the identification

Address for reprint requests and other correspondence: A. Colosimo, Dipartimento di Scienze Biochimiche, A. Rossi Fanelli, Università Degli Studi di Roma La Sapienza, Piazzale Aldo Moro, 5, 00185 Rome, Italy (E-mail: colosimo@caspur.it).

The costs of publication of this article were defrayed in part by the payment of page charges. The article must therefore be hereby marked "*advertisement*" in accordance with 18 U.S.C. Section 1734 solely to indicate this fact.

of reliable mechanistic models. Moreover, we complemented the statistical description of TEOAE dynamics by analyzing the properties of single signals through a singular value decomposition (SVD) approach that makes it possible to estimate the basic modes generating TEOAEs, as well as to verify the congruence between natural and simulated systems. This approach is absolutely new in the study of TEOAE signals and opened the door to relevant conclusions concerning *1*) the individual features of TEOAE responses, which are not significantly different between the studied age groups; and *2*) the basic difference between natural and simulated signals in terms of number of normal modes buried in them.

MATERIALS AND METHODS

Data Sets

Neonatal TEOAE responses. The neonatal TEOAE responses were collected in a quiet room of the Neonatology department of Ferrara University, Italy, in the second day of life (48 h) and during spontaneous sleep after feeding, according to protocols described in previous publications (12, 13, 27). The 60 newborn subjects were randomly selected and were characterized by a normal weight (3.2–4.0 kg) and an Apgar index of neurological development and health higher than 8 and did not present any audiological risk factors. All of the responses selected for the present work showed a TEOAE correlation ≥80%, a value established in previous studies (12, 22, 23) as the criterion for accepting the normality of a neonatal TEOAE response.

The TEOAE responses were recorded by the Otodynamics ILO-292 analyzer (software version 4.20B and 5.60H). The standard Institute of Laryngology and Otology (ILO) TEOAE neonatal probe was employed in all recordings. The adequacy of the probe fit was evaluated by measuring the proper frequency range of the stimulus (1.0–5 kHz).

TEOAE responses from adult subjects. The adult TEOAE responses were obtained in the Audiology department of Palermo University, Italy, from 62 subjects, chosen on the basis of the absence of *1*) any pathophysiologically objective sign of clinical relevance, and *2*) any systematic pharmacological treatment within 3 mo from the acquisition of the TEOAE response. Click-evoked emissions were recorded in a sound-attenuated booth with the patient seating adjacent to the recording equipment by using an ILO88 system (Otodynamics) with standard adult ILO probes. The probe fit was evaluated by measuring the adequacy of the stimulus across the frequency range of 0.5–5 kHz.

TEOAE Protocols

For both neonatal and adult subjects, a nonlinear TEOAE stimulation protocol was used, consisting of three clicks with a positive polarity, followed by a fourth click with inverse polarity and intensity equal to the sum of the previous three. For the neonatal subjects, the click stimuli had an intensity of 82- to 84-dB sound pressure level; for the adult subjects, stimuli of 76- to 80-dB sound pressure level were used.

The responses were high-pass filtered at 500 Hz (adults) and 1,200 Hz (neonates). Because of time restrictions in the Neonatology ward, the neonatal responses were the average of at least 100 individual responses (sweeps). When the signal-to-noise ratio at 2.0, 3.0, and 4.0 kHz was higher than 8.0, 11.0, and 10.0 dB, respectively (12), the neonatal TEOAE response was considered a "pass," and the subject was added to the pool of acceptable subjects. For the adult subjects, each response was the average of a minimum of 260 to a maximum of 2,400 individual sweeps. A response was considered a pass when the signal-to-noise ratio was higher than 3 dB at 2.0, 3.0, and 4.0 kHz (10, 24, 28).

RQA Parameters

RQA aims for a direct and quantitative description of the amount of deterministic structure (5, 29) of a signal, and it was shown to be an efficient and relatively simple tool in the nonlinear analysis of many physiological signals (4, 8, 30, 32). The basic idea behind RQA is the identification of recurrence of local data points in a reconstructed phase space. The targeted system is analyzed by reconstructing the space of the true signal dynamics, by using a coordinate system of surrogate variables, created by a combination of the measured signal and time-lagged copies of itself. In this work, the temporal series delay (lag) has been set to 1.

This coordinate system (embedding matrix) is then transformed into a distance matrix by simply computing the Euclidean distance between rows (epochs) of the embedding matrix. An important aspect of the RQA is the definition of *1*) the embedding dimension for the deconvolution of the original signal in a multidimensional space, and *2*) the radius (maximum euclidean distance at and below which the recurrent points are defined and displayed) (6, 18, 20, 35–37).

Each distance below the radius is considered a recurrence pair, and the distance matrix is transformed into a recurrence plot by darkening all of the recurrent points (Fig. 1, *C* and *D*).

For the adult and neonatal data sets, the following RQA parameter values have been used, as suggested in a previous study (38): embedding dimension = 10 and radius = 15. This last value is expressed as a percentage of the average distance among all epochs and automatically scales for any differences in the TEOAE signal amplitude.

The RQA descriptors used in this study are the following. The first is the percentage of recurrence, which quantifies the percentage of the plot occupied by recurrent points.

The second is the percentage of determinism (%Det), which is the percentage of recurrent points that appear in a sequence, forming diagonal line structures in the distance matrix. A line is defined a priori as the sequence that is equal to or longer than a predetermined threshold length. In the present case, the threshold was set to 8. In this context, the radius parameter defines the distance below which two epochs are considered recurrent, and the %Det threshold defines the minimum number of consecutive recurrent points that can be scored as deterministic.

The %Det corresponds to the number of patches of recurrent behavior in the studied series, i.e., to portions of the state space in which the system resides for a longer duration than expected by chance alone [quasi-attractors (34)]. It should be noted that, theoretically, a recurrence can be observed by chance whenever the system explores two nearby points of its state space. On the contrary, the observation of recurrent points that are consecutive in time and that form lines parallel to the main diagonal is an important signature of deterministic structuring (5, 31, 32).

The third RQA descriptor is the entropy, which is defined in terms of the Shannon-Weaver formula for information entropy (32) computed over the distribution of length of the lines of recurrent points and measures the richness of deterministic structuring of the series.

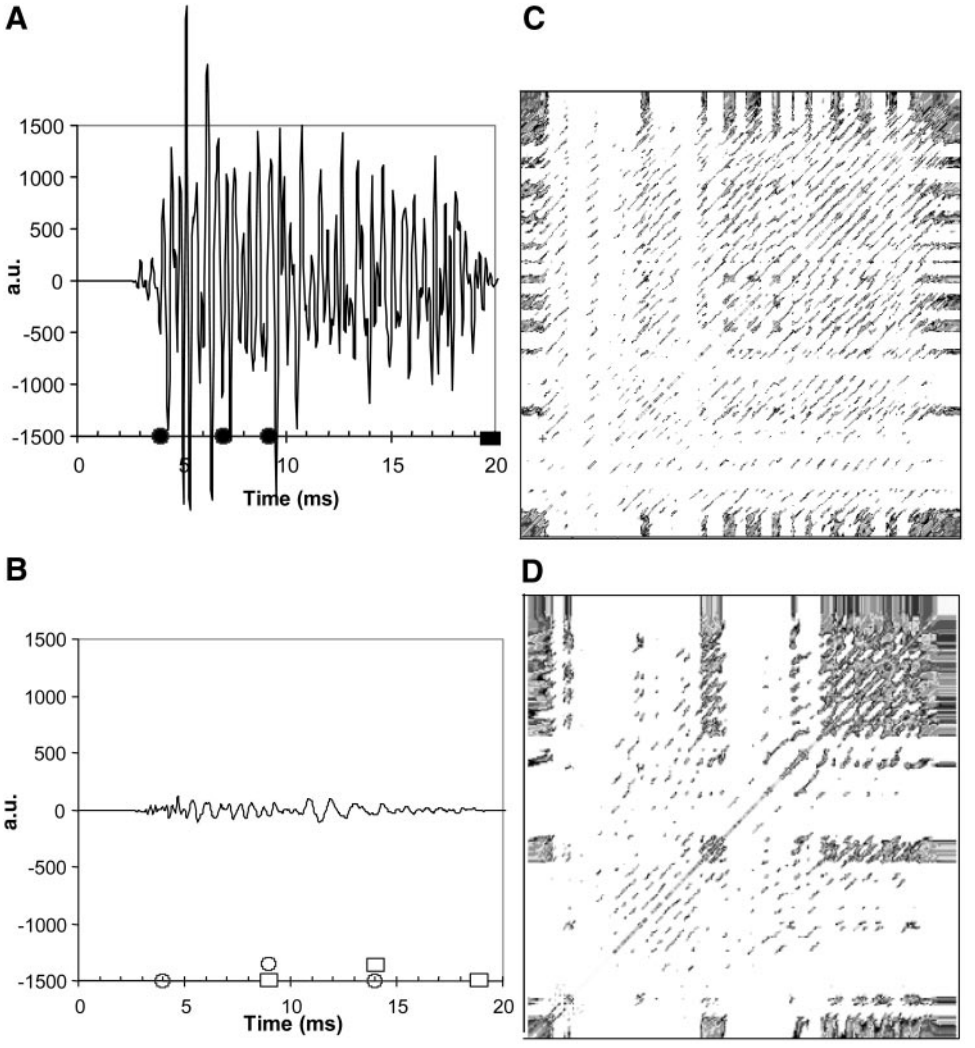

Fig. 1. Typical transiently otoacoustic emission (TEOAE) signals and their recurrence plots. *A* and *C*: typical TEOAE signal from a newborn and the corresponding recurrence plot, respectively. *B* and *D*: an adult signal and the corresponding recurrence plot, respectively. *A* and *B*: solid and open symbols show, respectively, overlapping (T1, T2, T3) and nonoverlapping (P1, P2, P3) windows. See MATERIALS AND METHODS for further details. Circles and squares indicate, respectively, the start and the end of windows. *C* and *D*: the used recurrence quantification analysis (RQA) parameters are embedding = 10, radius = 15, lag = 1, line = 8. au, Arbitrary units.

Based on data from a previous study (38), the %Det appears as the parameter of choice because of its higher content of robust information concerning the dynamic structure of the analyzed responses.

The %Det variable was studied in terms of population properties and on an individual basis. For the population analysis, we compared the two age groups, looking for the existence of a significant difference in the amount of determinism. This comparison, performed on different time windows, allowed us to evaluate *1*) the amount of stationarity along the various segments of the TEOAE response, and *2*) the stationarity differences between the two groups. For the individual analysis, more than one response was available for a number of subjects. From these repetitions, we could compute the value of inter- and intraindividual variability in the %Det variable, as well in other RQA descriptors. From the ratio of intra- and intersubject variability, we were able to estimate the average amount of "individuality" within the two age groups.

PCA and SVD

PCA and SVD are two applications of essentially the same algorithm, designed to solve an eigenvalue and/or eigenvector problem, in different contexts (20).

PCA has been proven most useful in multivariate statistics as a means to minimize redundant information (14), whereas SVD is used to identify the essential dynamic modes of time-dependent signals (1–3), acting as a precise noise-filter tool. PCA applies to data sets having the form of a rectangular matrix $\mathbf{X}$, where the rows are the statistical units (M) and the columns are the measured (or observed) variables (N). In the case of SVD, the matrix $\mathbf{X}$ has subsequent time-lagged copies of a time series as columns and subsequent epochs of length equal to the embedding dimension as rows. The matrix $\mathbf{X}$ can be expressed as

$$\mathbf{X} = \mathbf{U}\,\mathbf{S}\,\mathbf{V}^{\mathrm{T}} \qquad (1)$$

where T indicates a transposed matrix; the matrices $\mathbf{U}$ and $\mathbf{V}$ have dimensions M × K and N × K, respectively, and fulfill the relation $\mathbf{U}^{\mathrm{T}}\,\mathbf{U} = \mathbf{V}^{\mathrm{T}}\,\mathbf{V} = 1$; and $\mathbf{S}$ is a K × K diagonal matrix whose nonzero elements (singular values) are such that $s_{11} > s_{22} > s_{33} \ldots > s_{kk} > 0$.

Within this context, we can project the original data into a new set of coordinates $\mathbf{US}$ (principal component scores) with no loss of information. Each element of $\mathbf{X}$ can, in fact, be reconstructed by the equation

$$\mathbf{X}_{ij} = \sum_{k=1\ \mathrm{to}\ \mathrm{N}} \mathbf{U}_{ik}\,\mathbf{S}_{k}\,\mathbf{V}_{jk} \qquad (2)$$

The new coordinates are by construction orthogonal (i.e., statistically independent), with each representing an independent aspect of the data set.

PCA is one of the most widespread modeling techniques, with applications ranging from sociology to organic chemistry, physiology, and theoretical physics, thanks to the following property: by an expansion truncated to A terms (with A < N), one obtains

$$\mathbf{X}_{ij} = \sum_{k=1 \text{ to A}} \mathbf{U}_{ik}\, \mathbf{S}_k\, \mathbf{V}_{jk} + E^2_{ij} \quad (3)$$

where the squared error term (E^2_{ij}) is a minimum. What makes *Eq. 3* different from *Eq. 2* is the presence of the error term and the sum limited to a lower number of coordinates with respect to the original data field. Because the error term is a minimum, projecting the original data on the new, lower dimensional component space (A < N) is optimal in a least squares sense. This implies that we can keep the meaningful (signal-like) part of the information, contained in the first principal components, and discard the noise, contained in the error term. In the PCA context, "meaningful" means "correlated," because the first principal components convey information linked to the correlated portion of the information carried by each variable, whereas the (uncorrelated) noise remains confined within minor components.

By the SVD method, a privileged coordinate system is obtained by diagonalizing a correlation matrix in an embedding space (3–4). The method points to the determination of the approximate number of modes (eigenvalues) excited in the system. In particular, from the percentage of variance explained by each eigenvalue, the number of independent (orthogonal) modes structuring the overall dynamics may be estimated. Moreover, the number of significant eigenvalues is a measure of the complexity of the system comparable to the correlation dimension.

In the present study, we applied both PCA and SVD. PCA was used to investigate the amount of individuality in terms of clusters of repeated TEOAEs from the same individuals in a component space derived from RQA parameters, and SVD was applied to single TEOAE signals to compute their relative complexity in terms of the number of normal modes necessary to attain a given level of explained variability.

TEOAE Simulation

To synthesize the TEOAE responses, we have assumed that the inner ear behaves as a bank of gammatone filters and that a click-evoked otoacoustic emission is simply the sum of the impulse responses generated by each filter. The gammatone simulation method has been chosen because of the relatively easy interpretation and physiological meaning of the simulated results. Each gammatone generator behaves as a narrow band-pass filter and is characterized by a specific central frequency (f_c), which varies along the basilar membrane and is inversely proportional to the distance from the stapes. In the time domain, each gammatone (γ) is given by

$$\gamma(t) = a t^3\, e^{-\beta\omega c t} \cos \omega_c\, t \quad (4)$$

where t is time, $\omega_c = 2\pi f_c$, $b = \beta\omega_c$ is even related to the signal damping (see Fig. 5), and $a = (\omega_c)^{3.5}$ makes the power of the gammatone independent of ω_c (Ref. 33 and references therein).

We used a set of five gammatones as suggested by Wit et al. (33), with f_c set at 1.0, 1.5, 2.2, 3.3, and 5.0 kHz, and a reduced set including three elements with f_c values located at the extreme and in the middle of the frequency range between 1.5 to 5 kHz (f_c set at 1.0, 2.2, and 5.0 kHz).

The aim of the simulations was to investigate whether the overall similarity in the TEOAE waveform shape was matched by similar results of the SVD analysis for natural and simulated signals.

RESULTS

Comparing Adult and Neonatal Responses in Different Time Windows

Considering that the default ILO response has a length of 20.4 ms, several smaller windows were studied. Such an approach revealed important information regarding *1*) the study of stationarity for signals from both data sets, and *2*) the identification of the window that best discriminates neonatal and adult TEOAE responses.

The RQA was carried out within three overlapping time windows (T1, T2, and T3) having different starting points (from 4.0, 7.0, and 9.2 ms, respectively) and a common ending point of 20 ms (see Fig. 1*A*). These windows were chosen according to the following considerations. In the first 4 ms (T1), the adult signals have an amplitude of almost zero (13). In the adult subjects, the most significant part of the responses (13, 27) occurs after 7 ms (T2). After 10 ms (T3), the signal's amplitude decreases abruptly, and low-frequency components appear.

To attain a more precise estimate among the responses at different time intervals and to localize the time occurrence of nonstationarities in the two age classes, the analysis was also carried out over three identical but nonoverlapping 5-ms segments. These windows were named P1 (4.0–9.0 ms), P2 (9.0–14.0 ms), and P3 (14.0–19.0 ms) and are shown in Fig. 1*B*.

The data in Fig. 2 show that, for all of the six considered windows, the %Det values in the neonatal

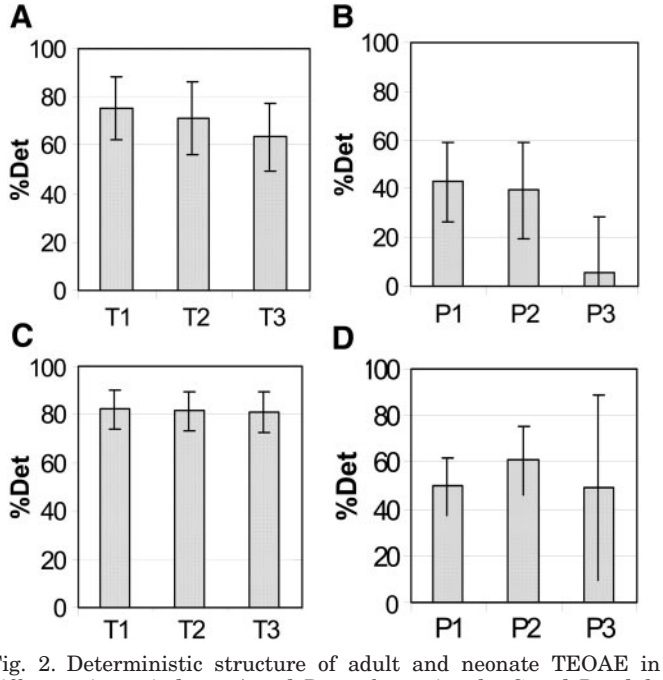

Fig. 2. Deterministic structure of adult and neonate TEOAE in different time windows. *A* and *B*: newborn signals; *C* and *D*: adult signals. *A* and *C*: overlapping time windows; *B* and *D*: nonoverlapping time windows. The time spans of the windows are as follows: T1 = 4–20 ms; T2 = 7–20 ms; T3 = 9.2–20 ms; P1 = 4–9 ms; P2 = 9–14 ms; P3 = 14–19 ms. Values are means ± SD. %Det, percentage of determinism.

group (Fig. 2, *A* and *B*) are lower than those from the adult subjects (Fig. 2, *C* and *D*); the differences between the two age classes, however, were more evident in nonoverlapping windows. To provide a conservative estimate of such differences, in all subsequent analyses we only considered overlapping windows. The RQA parameters were calculated in the T2 time window because the corresponding standard deviation values of the intersubject variability were maximal.

Individual Features

The analysis of the %Det variable showed that the intersubject variability was larger in neonates than in adults, in accordance with the information in the literature (11, 25). Also, the intrasubject variability was larger in neonates than in adults. On the contrary, the "extent" of individual features, as indicated by the ratio of intersubject to intrasubject variability, presented similar values, as shown in Table 1.

The analysis of the Pearson correlation coefficient between two waveforms × 100 (Repro variable) produced different results. For the adult responses, the extent of individual features was estimated as 2.87/0.81 = 3.56, whereas, in the case of neonatal responses, the estimated value was 2.43/2.20 = 1.10. Such an estimate fails to highlight any individual character for the Repro value in the neonatal group, pointing to a relative weakness of the Repro parameter in the evaluation of acoustic performance of newborns, due to a relevant intrasubject variability.

Data from a previous study showed that replicated TEOAE responses from adult subjects are recognizable in a principal component space (38), namely, that responses recorded from the same subject fall close to each other in a principal component reference plane. More precisely, signals from the same ear of the same subject and analyzed by RQA cluster in a principal component reference plane derived from the percentage of recurrence, %Det, and entropy parameters. The same procedure has been applied in the present study to sort out individual features in both neonates and adults. In Fig. 3, it is possible to observe that signals recorded from the same ear of the same subject cluster in a principal component reference plane derived from the RQA descriptors. In the case of adults, it was also possible to test the reliability of these results by using signals recorded in subsequent sessions.

Table 1. *Inter- and intrasubject variability in %Det*

	Inter	Intra	Inter/Intra
Neonates	15.64	4.22	3.70
Adults	9.91	2.61	3.79

Average and standard deviation values of percentage of determinism (%Det) over repeated signals of the same individual are calculated for at least 6 individuals in each age class. Intersubject variability (Inter) is the standard deviation of the averages relative to individuals in the same class. Intrasubject variability (Intra) is the average of the standard deviations between different registrations relative to the same individual. Inter/Intra, ratio of Inter to Intra.

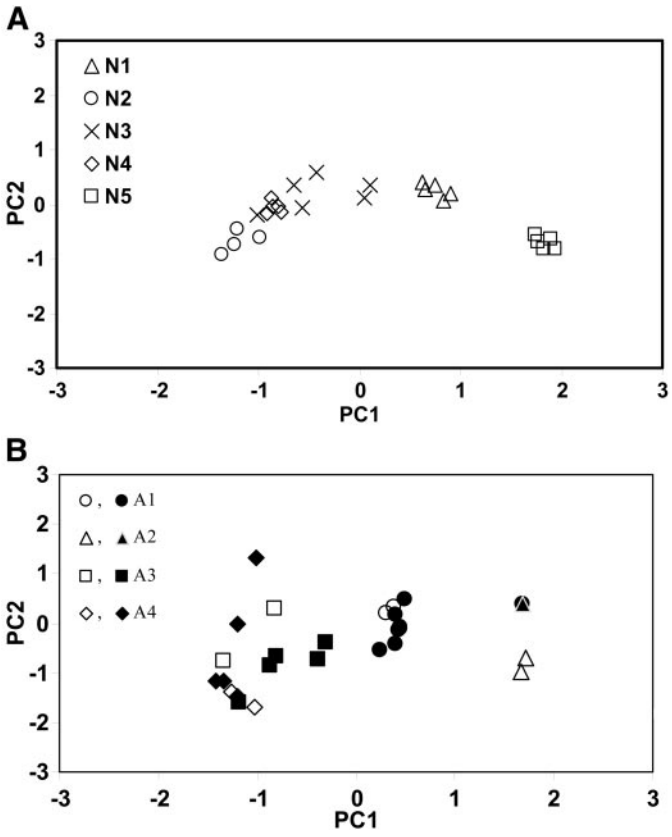

Fig. 3. TEOAE clustering in a principal component (PC) analysis (PCA) plane. *A*: neonate left ear signals. *B*: adult left ear signals. The PCA was carried out over the main RQA parameters (percentage of recurrence, %Det, entropy). In both panels, the same symbol is used for the same individual. *B*: solid symbols refer to signals recorded for a given individual in subsequent experimental sessions, separately analyzed and plotted over the plane obtained by an initial (learning) set of measurements (open symbols). N1–N5, *neonates 1–5*; A1–A4, *adults 1–4*.

SVD Analysis of Natural and Simulated TEOAE Signals

Figure 4 reports the distribution of the total average variability explained by each mode within a subset of at least 10 adult and neonatal responses. A relevant feature emerging from this analysis is that, in both data sets, the majority (90–95%) of the observed variability is explained by four eigenvalues arranged into couples. This suggests that the responses of both data sets might contain components from four classes of TEOAE generators, divided into two pairs. In each pair, the constituent elements oscillate, on the average, with a phase shift of ~90° (sine-cosine pairing) with respect to each other.

Figure 5 reports the results obtained over the simulated TEOAE signals with a three- and a five-gammatone model. For both models, the SVD analysis was carried out by using slightly different values of β. This parameter is inversely proportional to the filter "gain," namely to the active (amplifying) function of the gammatone. Fig. 5, *A* and *B*, shows the simulated TEOAEs based on three and five gammatones, respectively; Fig.

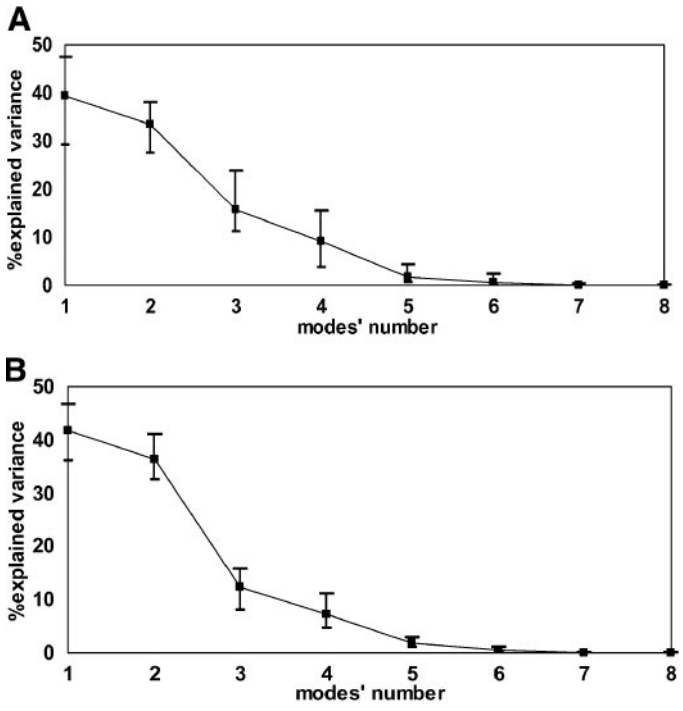

Fig. 4. Singular value decomposition analysis of real TEOAE signals. *A*: responses from adult subjects. *B*: responses from neonatal subjects. For each group, average values were estimated from at least 10 signals and reported, for both classes, together with maximum and minimum values. Values are means ± SD.

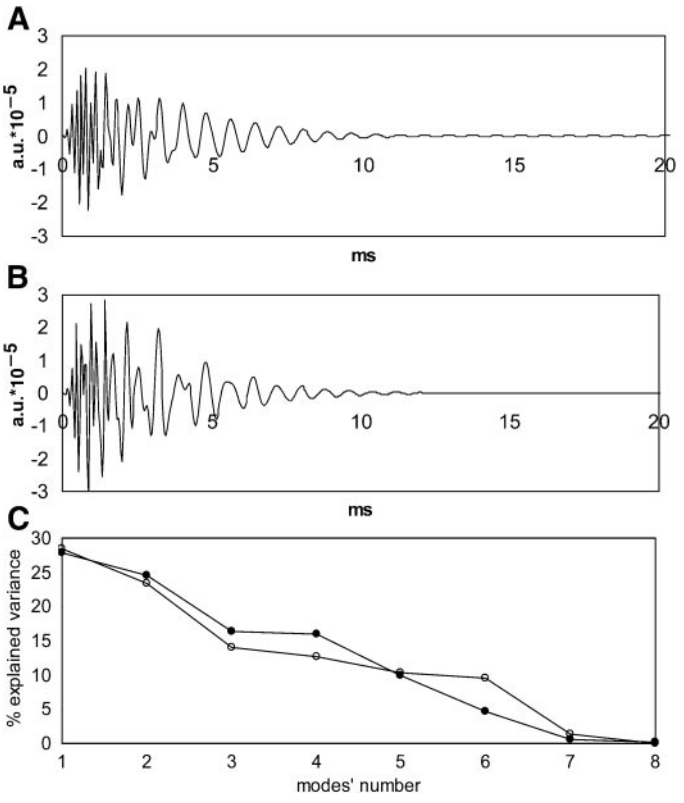

Fig. 5. Simulated TEOAE signals. Simulated TEOAE are from 3- and 5-component gammatone model: *A*: 3-component model with central frequency set at 1.0, 2.2, and 5.0 kHz and $\beta = 0.1$. *B*: 5-component model with central frequency set at 1.0, 1.5, 2.2, 3.3, and 5.0 kHz and $\beta = 0.11$; *C*: singular value decomposition analysis of the simulated TEOAE signals in *A* (●) and *B* (○). For the meaning of β, see the text.

5*C* reports the SVD analysis of the two simulated signals.

The number of essential modes associated with both of the simulated signals is basically the same (6) and significantly higher than the one observed in natural signals (Fig. 4). Concerning the distribution of the percentage of the explained variance over the mode's number, the TEOAE signal generated by three gammatones (Fig. 5*A*) seems to better reproduce the characteristic coupling of the natural signals. The total variance explained by modes 1–5 is >99.0% for both newborn and adult signals and is 94.7 and 89.0% in the case of signal simulated by three and five gammatones, respectively. Despite the obvious limitations of the model, this points to a relatively simple behavior of the natural system under the explored conditions.

DISCUSSION

Comparing neonatal and adult TEOAE responses revealed a number of dynamic differences and similarities, which can be summarized as follows.

First, the newborn responses appear less deterministic than the adult ones in all of the investigated conditions in the overlapping windows (T1, T2, T3), as well as in the nonoverlapping windows (P1, P2, P3). We assume that the decrease of the variable %Det in the neonatal responses of the P3 window (14–19 ms) might be related to the lack of medium-low TEOAE frequencies generated by apical OHCs, which are supposed to be mainly responsible for the last portion of the signal (12, 13, 28).

Second, the responses from neonatal subjects are less stationary compared with those from adults. The nonoverlapping windows P1–P3 highlighted a small, albeit statistically significant, difference between the two groups in terms of the relative stationarity character of TEOAEs. Based on these results, it might be speculated that the adult signals were more structured; in this context, the aging processes of the auditory periphery can be considered as a progressive and system-ordering process.

Third, both adult and neonatal TEOAE responses show the same amount of individual features, as measured by the ratio between inter- and intrasubject

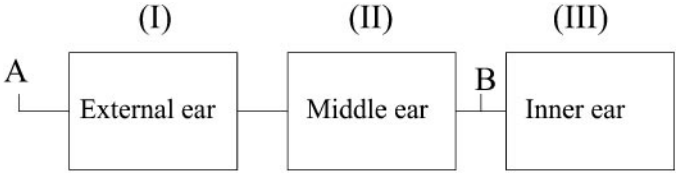

Fig. 6. Block scheme of the auditory system. *Point A* indicates the microphone position in the experimental setup for TEOAE recording. The pathway of the natural TEOAEs from generation to the monitoring site is from III to II to I. *Point B* shows the round window location of the inner ear, where in theory the simulated signals should be observed.

variability of the %Det variable. Although the inter- and intrasubject variabilities are different in the two data sets, the ratio value is quite similar (3.70 vs. 3.79 for adults and neonates, respectively). This implies that individual characteristics are present in the TEOAE responses since the first days of life. These results were also confirmed by PCA on the entire set of RQA parameters and fast Fourier transform spectral parameters (5 values, 1 for each frequency bands; results not shown).

Fourth, both data sets display the same number of dominant modes as shown by SVD analysis. This result suggests that the dynamic features of the TEOAE responses are similar for both age groups. Differences were observed between natural and simulated TEOAE responses: the latter show a higher complexity (more modes were needed to explain the same percentage of variability), which is probably caused by the lack of coupling between the structures responsible for the number of modes.

In general, the results indicate an overall decrease in complexity from neonatal to adult TEOAE responses. This decrease involves a signal regularization (increase in stationarity), as well as a higher determinism. Within this context, it might be hypothesized that the aging process makes the TEOAEs more similar between them (lower interindividual variability) and more stable. Concerning individuality, the similarities between the two groups are in agreement with a genetic source of intersubject variability. On the other hand, genetic factors, being age independent, cannot account for the differences observed between the age groups (loss of complexity, stationarity increase, etc.). Thus, in such a case, functional and/or physiological explanations are in order.

In such a context, it may be useful to identify the biological structures responsible for the "principal modes" of the natural TEOAEs shown in Fig. 4, on the basis of the scheme of Giguere and Woodland (7, 21) reported in Fig. 6.

The simulated TEOAE signal in Fig. 5 can be considered the output of the cochlear amplifier at the level of the round window, and in this context the simulated response (Fig. 6, *point B* in the scheme) is not filtered by the transfer functions of both the middle and the external ear. Real TEOAE responses of the type shown in Fig. 1 were recorded inside the auditory canal (*point A* in Fig. 6). The difference in dominant modes between real and simulate responses suggests that *blocks I* and *II* of Fig. 6 are somehow responsible for reducing the TEOAE complexity.

As for the source of individual features, it should be noted that our analysis is independent of the TEOAE response amplitude, which rules out trivial considerations based on different ear size or morphology. Identical results as those reported in Fig. 3 (data from left ear responses) were obtained from right ear responses (not shown). It seems relevant to notice that the number of dominant modes is essentially identical in newborn and adult signals; this indicates that, whatever the mechanistic basis of the underlying phenomena would be, it does not reveal any age-dependent effect under our conditions. We could not find any significant correlation between signals from the two ears of the same subject. Thus the mechanistic source of TEOAE individual features should be searched on a microscale, maybe at the level of different distribution patterns of OHCs, which could be envisaged as different in the two ears, even for newborns. This point, however, surely needs more detailed investigation. The comparison between preterm and full-term newborns seems also worthy of investigation in future works. In both cases, as well as in any other analytic study of TEOAE signals, it is difficult to overestimate the heuristic power of simulated signals generated by appropriate mechanistic models (15, 16). As indicated by the simulation results reported in the present study on the basis of a relatively simple model, however, such an approach, if aiming to account for the subtle dynamic features of TEOAEs at the highest possible level of resolution, requires consideration of the possible nonlinear coupling between the functional units included in the underlying mechanism.

The authors are indebted to Maddalena Rossi (University of Ferrara) for TEOAE data collection and to Prof. G. Grisanti and Dr. C. Parlapiano (University of Palermo) for data collection and very useful discussions.

This work has been partly supported by grants of the Italian Ministero dell' Università e della Ricerca Scientifica e Tecnologica (60%) to A. Colosimo.

REFERENCES

1. **Bartholomew DJ.** The foundation of factor analysis. *Biometrika* 71: 221–232, 1984.
2. **Bertero M and Pike ER.** Signal processing for linear instrumental systems with noise. In: *Signal Processing and Its Applications,* edited by Bose NK and Rao CR. Amsterdam: North Holland, 1993, vol. 10, p. 1–46.
3. **Broomhead DS and King GP.** Extracting qualitative dynamics from experimental data. *Physica D* 20: 217–236, 1986.
4. **Colosimo A, Giuliani A, Mancini AM, Piccirillo G, and Marigliano V.** Estimating a cardiac age by means of heart rate variability. *Am J Physiol Heart Circ Physiol* 273: H1841–H1847, 1997.
5. **Eckmann JP, Kamphorst SO, and Ruelle D.** Recurrence plots of dynamical systems. *Europhys Lett* 4: 973–977, 1987.
6. **Gao J and Cai H.** On the structures and quantification of recurrence plots. *Phys Lett A* 270: 75–87, 2000.
7. **Giguere GC and Woodland PC.** A computational model of the auditory periphery for speech and hearing research. I. Ascending path. *J Acoust Soc Am* 95: 331–342, 1994.
8. **Giuliani A, Piccirillo G, Marigliano V, and Colosimo A.** A nonlinear explanation of aging-induced changes in heartbeat dynamics. *Am J Physiol Heart Circ Physiol* 275: H1455–H1461, 1998.
9. **Giuliani A, Sirabella P, Benigni R, and Colosimo A.** Mapping protein sequence spaces by recurrence quantification analysis: a case study on chimeric structures. *Protein Eng* 13: 671–678, 2000.
10. **Grandori F and Ravazzani P.** Non-linearities of click-evoked otoacoustic emissions and the derived non-linear technique. *Br J Audiol* 27: 97–102, 1993.
11. **Harrison WA and Norton SJ.** Characteristics of transient evoked otoacoustic emissions in normal-hearing and hearing-impaired children. *Ear Hear* 20: 75–86, 1999.
12. **Hatzopoulos S, Petruccelli J, Pelosi G, and Martini A.** A TEOAE screening protocol based on linear click stimuli: performance and scoring criteria (Abstract). *Acta Otolaryngol* 119: 135, 1999.

13. **Hatzopoulos S, Tsakanikos M, Grzanka A, Ratynska J, and Martini A.** A comparison of neonatal TEOAE responses recorded with linear and QuickScreen protocols. *Audiology* 39: 70–79, 2000.
14. **Hol PG, Port SC, and Stone CJ.** *Introduction to Statistical Theory.* Boston, MA: Houghton Mifflin, 1971.
15. **Kapadia S and Lutman ME.** Nonlinear temporal interactions in click-evoked otoacustic emissions. I. Assumed model and polarity-symmetry. *Hear Res* 146: 89–100, 2000.
16. **Kapadia S and Lutman ME.** Nonlinear temporal interactions in click-evoked otoacustic emissions. II. Experimental data. *Hear Res* 146: 101–120, 2000.
17. **Kon K, Inagaki M, and Kaga M.** Developmental changes of distortion products and transient evoked otoacoustic emissions in different age groups. *Brain Dev* 22: 41–46, 2000.
18. **Manetti C, Ceruso MA, Giuliani A, Webber CL, and Zbilut JP.** Recurrence quantification analysis as a tool for characterization of molecular dynamics simulation. *Phys Rev E* 59: 992–998, 1999.
19. **Maxon AB, Vohr BR, and White KR.** Newborn hearing screening: comparison of a simplified otoacoustic emissions device (ILO1088) with the ILO88. *Early Hum Dev* 45: 171–178, 1996.
20. **Meloun M, Capek J, Miksik P, and Brereton RG.** Critical comparison of methods predicting the number of components in spectroscopic data. *Anal Chim Acta* 423: 51–68, 2000.
21. **Merhaut J.** *Theory of Electroacoustics.* New York: McGraw-Hill Int, 1981.
22. **Morand N, Khalfa S, Ravazzani P, Tognola G, Grandori F, Durrant JD, Collet L, and Veuillet E.** Frequency and temporal analysis of contralateral acoustic stimulation on evoked otoacoustic emissions in humans. *Hear Res* 145: 52–58, 2000.
23. **Morlet T, Goforth L, Hood LJ, Ferber C, Duclaux R, and Berlin CI.** Development of human cochlear active mechanism asymmetry: involvement of the medial olivocochlear system? *Hear Res* 137: 179–189, 1999.
24. **Morlet T, Micheyl C, Giraud AL, Collet L, and Morgon A.** Contralateral suppression of evoked otoacoustic emissions and detection of a multi-tone complex in noise. *Acta Otolaryngol* 115: 178–182, 1995.
25. **Norton SJ.** Application of transient evoked otoacoustic emissions to pediatric populations. *Ear Hear* 14: 64–73, 1993.
26. **Norton SJ, Gorga MP, Widen JE, Folsom RC, Sininger Y, Cone-Wesson B, Vohr BR, Mascher K, and Fletcher K.** Identification of neonatal hearing impairment: evaluation of transient evoked otoacoustic emission, distortion product otoacoustic emission, and auditory brain stem response test performance. *Ear Hear* 2: 508–528, 2000.
27. **Pelosi G, Hatzopoulos S, Chierici R, Vigi V, and Martini A.** Valutazione di un protocollo TEOAE lineare nello screening audiologico neonatale: studio di fattibilità. *Acta Otorhinolaryngol Ital* 18: 213–217, 1998.
28. **Probst R, Lonsbury-Martin BL, and Martin GK.** A review of otoacoustic emissions. *J Acoust Soc Am* 89: 2027–2067, 1991.
29. **Provenzale A, Smith LA, Vio R, and Murante G.** Distinguishing between low-dimensional dynamics and randomness in measured time series. *Physica D* 58: 31–49, 1992.
30. **Riley MA, Balasubramaniam R, and Turvey MT.** Recurrence quantification analysis of postural fluctuations. *Gait Posture* 9: 65–78, 1999.
31. **Trulla LL, Zbilut JP, Giuliani A, and Webber CL.** Recurrence quantification analysis of the logistic equation with transient. *Phys Lett A* 223: 255–260, 1996.
32. **Webber CL and Zbilut JP.** Dynamical assessment of physiological systems and states using recurrence plot strategy (Abstract). *J Appl Physiol* 76: 965, 1994.
33. **Wit HP, van Dijk P, and Avan P.** Wavelet analysis of real ear and synthesized click-evoked otoacoustic emissions. *Hear Res* 73: 141–147, 1994.
34. **Zak M, Zbilut JP, and Meyers RE.** *From Instability to Intelligence. Lecture Notes in Physics.* Heidelberg, Germany: Springer, 1997.
35. **Zbilut JP, Giuliani A, and Webber CL.** Recurrence quantification analysis and principal components in detection of short complex signals. *Phys Lett A* 237: 131–135, 1998.
36. **Zbilut JP, Giuliani A, Webber CL, and Colosimo A.** Recurrence quantification analysis in structure-function relationship of proteins: an overview of a general methodology applied to the case of TEM-1 beta lactamase. *Protein Eng* 11: 87–93, 1998.
37. **Zbilut JP, Webber CL Jr, Colosimo A, and Giuliani A.** The role of hydrophobicity patterns in prion folding as revealed by recurrence quantification analysis of primary structures. *Protein Eng* 13: 99–104, 2000.
38. **Zimatore G, Giuliani A, Parlapiano C, Grisanti G, and Colosimo A.** Revealing deterministic structures in click-evoked otoacoustic emissions. *J Appl Physiol* 88: 1431–1437, 2000.